

Improvement of Power System Transient Stability Using an Intelligent Control Method

Mohsen Darabian, Bahram Khorram, Mehdi Azari

Abstract— Shunt Flexible AC Transmission System (FACTS) devices, when placed at the mid-point of a long transmission line, play an important role in controlling the reactive power flow to the power network and hence both the system voltage fluctuations and transient stability. In this paper, a new intelligent controller used to control the output of an SVC to damp power system oscillations is developed. This controller is an online trained wavelet neural network controller (OTWNNC) with adaptive learning rates derived by the Lyapunov stability. Effectiveness of the proposed technique is robustness to different operating conditions and disturbances. The effectiveness of the proposed controllers is demonstrated on an 2-machine system. Results obtained show improvement in the overall system damping characteristics using the proposed method (OTWNNC).

Index Terms— Wavelet neural network (WNN), Particle Swarm Optimization (PSO), SVC Design, Transient stability.

I. INTRODUCTION

Power system stability (PSS) control is an important task in PSS operation [1]. Several factors, such as external disturbances or internal mechanical torques, may easily affect system stability. With the development of power electronics, the structural control of electric power networks has recently attracted more attention. In this context, flexible AC transmission system (FACTS) devices are becoming more popular. Due to their fast response, these devices are used to dynamically adjust the network configuration to enhance steady-state performance as well as dynamic stability [2]–[5]. The availability of FACTS devices, such as thyristor controlled series compensators (TCSCs), static var compensators (SVCs), and static synchronous series compensators (SSSCs), can provide variable turn and/or series compensation [3]. However, these devices can interfere with one another. When the controller parameters of a dynamic device are tuned to obtain the best performance, control conflicts that arise between various FACTS controllers may lead to the onset of oscillations [3, Ch. 9]. Thus, the coordinated control of these devices is very important [4]. TCSCs and SVCs have been widely studied in the technical literature and have been shown to

significantly enhance system stability [6]–[8]. Therefore, this paper employs these two devices and proposes a new coordinated control scheme to enhance the dynamic response of a multi-machine PSS.

Different FACTS device control methods have been proposed for power oscillation damping and transient stability improvement [9].

One popular damping control method uses a washout filter followed by an n th order lead-lag controller [10]–[14]. In general, the parameters of a lead lag controller are designed using the pole-zero location method [11], [12], [14]. Modern PSs are large-scale and complex. Disturbances typically change the network topology and result in a nonlinear response. Therefore, capabilities of traditional control laws based on linearized models are limited. To address this problem, FACTS control using fuzzy control scheme has been proposed [7-16]. Unlike previous control configurations, this paper proposes a fuzzy lead-lag control scheme for the control and coordination of TCSC and SVC devices in a multi-machine PS. In this new control configuration, an FC is designed to adaptively adjust the parameters of lead-lag controllers at each control time step. The performance advantage of the FACTS devices equipped with the fuzzy lead-lag controller is verified through comparison with traditional lead-lag controllers. Based on aforementioned before, a novel technique is very essential for the stabilization of power systems. Inspired algorithms such as Genetic Algorithm (GA) [17,18], Bacterial Foraging Optimization (BFO) [19] Artificial Bee Colony (ABC) algorithm [20] and Tabu Search (TS) [21] algorithm especially with stochastic search techniques have been employed to find optimal value of PSS stabilizer parameters. Recently, SO algorithm has become available and a promising technique for real world optimization problems. PSO as a population (swarm) based algorithms can solve a variety of difficulties associated with optimization problems. PSO applied to better stability of the power system

[22, 23,24,25,26]. In this paper is the application of an online trained wavelet neural network controller to provide the necessary control signal to the SVC so that power system oscillations are quickly damped out, since the Lyapunov stability method is used to guarantee the convergence of proposed controller, the overall control system is globally stable and hence, the transient stability of power system is improved; the control error can be reduced to zero by selecting appropriate parameters and learning rates; and the proposed controller can achieve favorable controlling performance. Meanwhile, no neural network identifier is used to approximate the dynamic of controlled power system.

Manuscript published on 30 April 2013.

* Correspondence Author (s)

Mohsen Darabian, MSc. student at Department of Electrical Engineering, University of Zanjan, Zanjan, Iran.

Bahram Khorram, Office of Standard and Industrial Research of Zanjan, Iran.

Mehdi Azari, MSc student at Department of Electrical Engineering, University of Zanjan, Zanjan, Iran.

© The Authors. Published by Blue Eyes Intelligence Engineering and Sciences Publication (BEIESP). This is an [open access](http://creativecommons.org/licenses/by-nc-nd/4.0/) article under the CC-BY-NC-ND license <http://creativecommons.org/licenses/by-nc-nd/4.0/>.

This paper is set out as follows: System model in Section II Problem statement is formulated in Section III. Heuristic optimization methods for solving the problem are presented in Section III. The application of the proposed model and simulation results are presented in Section V and finally, the conclusion is presented in Section VI.

II. SYSTEM MODEL

A. Power System Model

Fig. 1 shows a single-line diagram of the studied system Consisting of two machines and one large load center at bus3. The generation capacity of first power generation substation (G1) is 1000 MVA. The capacity of other one (G2) is 5000MVA. A large load is used to model the load center of approximately 6000MW. Both L1 and L2 are 350-kmlong. The SVC (400-MVAR) is placed at the generator

bus 2 to provide instantaneous reactive power modulation for voltage maintenance. The system data are given in the Table1andTable2. See Appendix A.

B. SVC Structure

SVC is basically a shunt connected static var generator/load whose output is adjusted to exchange capacitive or inductive current so as to maintain or control specific power system variables: typically, the controlled variable is the SVC bus voltage. One of the major reasons for installing a SVC is to improve dynamic voltage control and thus increase system load ability. An additional stabilizing signal, and supplementary control, superimposed on the voltage control loop of a SVC can provide damping of system oscillation as discussed in [27-28].

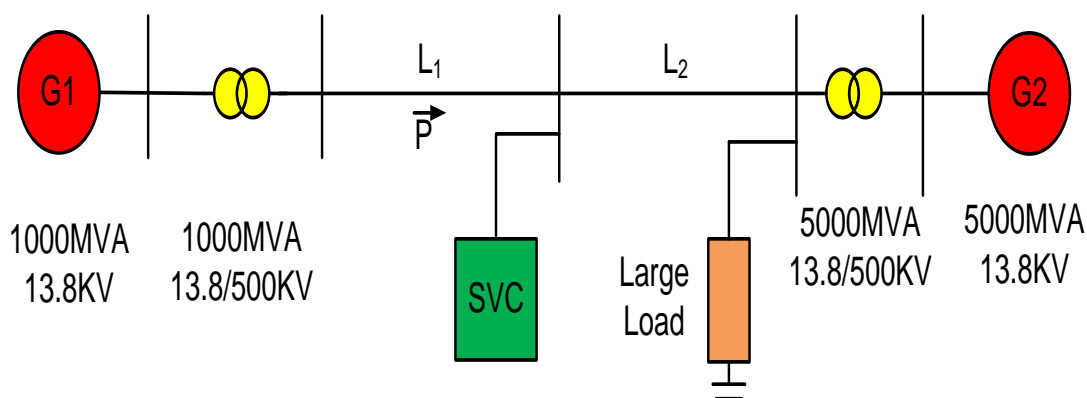


Fig1:Power system under study

Table1: The parameters used for G1 and G2

Parameters	Value	Parameters	Value
V_{L-L}	13.8kv	x'_q	0.50p.u
f	60HZ	x''_q	0.243p.u
r_a	0.003p.u	x_l	0.18p.u
x_d	1.305p.u	T'_{do}	1.01s
x'_d	0.296p.u	T''_{do}	0.053s
x''_d	0.252p.u	T''_{qo}	0.1s
x_q	0.474p.u	H	3.7

Table2: Parameters used for the excitation system

Parameters	Value	Parameters	Value
k_a	200p.u	k_f	0.001p.u
T_a	0.001s	T_f	0.1s
k_e	1p.u	E_{fmin}	-5p.u
T_e	0s	E_{fmax}	5p.u

III. PROPOSED METHOD

A. Online trained wavelet neural network controller (OTWNNC)

The proposed OTWNNC is shown in Fig.2. according to fig.2, the smart control system contains an online trained wavelet neural network controller. Also, computing block the active power transferred through the line L1 is obtained. The active Power output of the block is compared with a reference value P_{ref} . In fact, this reference value is equal to the active power transferred via L1 in steady-state of power system. According to figure 2, this error can be used as input

WNN. Finally, the output of this intelligent control system u is added to the reference voltage of SVC (V_{ref}). In order to determine the SVC susceptance B_{eq} for the maintaining voltage of voltage regulator is used (difference between the measured voltage V_m and the reference voltage ($V_{ref}+u$)). Therefore, the SVC regulates its output voltage based on the summation of the reference voltage and the output of the intelligent control system.

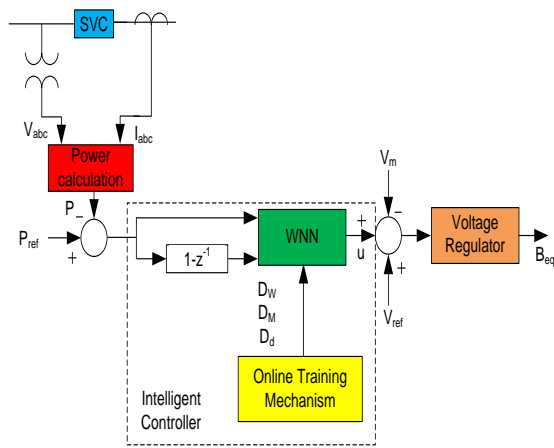


Fig.2:Block diagram of intelligent system

B. Wavelet neural network (WNN)

The wavelet neural network (WNN) contains three layers: input layer, hidden layer and output layer, a wavelet (the j layer) and an output layer is shown in Fig.3. The intelligent control system is designed to converge to zero error value. Therefore, the control error is defined as $e = (P_{ref} - P)$, in which P as shown in Fig.1 is the power transferred via L1. Also, desired value or reference of P is defined as P_{ref} which is equal to the value of the power transferred in the steady-state. In the wavelet layer, the output of each node is equal to equation (1); x_{ij}, m_{ij} and d_{ij} , are the input of WNN, the translation and dilation in j th term of the i th input x_i .

$$net_j = \sum_i^{N_i} \frac{x_i - m_{ij}}{d_{ij}} \quad (1)$$

$$\Phi_j = \phi(net_j)$$

The first derivative of a Gaussian function $\phi(x) = -x \cdot \exp(-0.5x^2)$ is chosen as a wavelet function. Hence, it can be said in the output layer, the overall output is equal to the summation of all input signals is expressed by equation (2); w_j is the connection weights between the wavelet layer and output layer.

$$u = \sum_{j=1}^{N_w} w_j \Phi_j \quad (2)$$

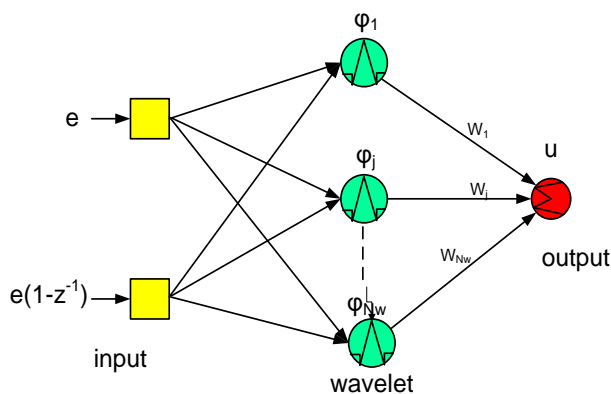


Fig.3:Structure of three-layer WNN

C. Online training mechanism

The proposed wavelet neural network model training algorithm is described as the calculation of a gradient vector in which each component in the training algorithm is defined as the derivative of a cost function with respect to parameters of WNN controller so that the cost function is minimized. Hence, the chain rule is used and the general method is referred as the back error propagation learning rule, since the gradient vector is computed in the direction opposite to the flow of the output of each node. The cost function is expressed by equation 3:

$$E = \frac{1}{2} e^2 = \frac{1}{2} (P_{ref} - P)^2 \quad (3)$$

According to general back-propagation algorithm [29], For the output layer, the error term to be propagated is computed as follows:

$$\delta_0 = -\frac{\partial E}{\partial u} = \left[-\frac{\partial E}{\partial e} \frac{\partial e}{\partial u} \right] = \left[-\frac{\partial E}{\partial e} \frac{\partial e}{\partial P} \frac{\partial P}{\partial u} \right] \quad (4)$$

Then update $W_j(k)$ by using $W_j(k+1)$ in backward computation of the WNN the following equation (5):

$$w_j(k+1) = w_j + \Delta w_j = w_j - \eta_w \frac{\partial E}{\partial w_j}$$

$$= w_j + \left[-\eta_w \frac{\partial E}{\partial u} \frac{\partial u}{\partial w_j} \right] = w_j + \eta_w \delta_0 \Phi_j \quad (5)$$

According to equation (5), η_w and k are the learning rate of the weight and the number of iteration. Since there is one neuron in the output layer, only the error term must be computed and propagated. So let this be equation (6):

$$\delta_j = -\frac{\partial E}{\partial net_j} = \left[-\frac{\partial E}{\partial u} \frac{\partial u}{\partial \Phi_j} \frac{\partial \Phi_j}{\partial net_j} \right] = \delta_0 w_j (net_j^2 - 1) \exp(-0.5net_j^2) \quad (6)$$

Also, update m_{ij} and d_{ij} are expressed by equation (7) and (8).

$$\Delta m_{ij} = -\eta_m \frac{\partial E}{\partial m_{ij}} = \left[-\eta_m \frac{\partial E}{\partial u} \frac{\partial u}{\partial \Phi_j} \frac{\partial \Phi_j}{\partial net_j} \frac{\partial net_j}{\partial m_{ij}} \right]$$

$$= -\eta_m \frac{\delta_j}{d_{ij}} \quad (7)$$

$$\Delta d_{ij} = -\eta_d \frac{\partial E}{\partial d_{ij}} = \left[-\eta_d \frac{\partial E}{\partial u} \frac{\partial u}{\partial \Phi_j} \frac{\partial \Phi_j}{\partial net_j} \frac{\partial net_j}{\partial d_{ij}} \right]$$

$$= -\eta_d \delta_j \frac{(x_i - m_{ij})}{(d_{ij})^2} \quad (8)$$

Finally, translation and dilation of the wavelet layer can be updated according to the following equations(9) and (10):

$$m_{ij}(k+1) = m_{ij}(k) + \Delta m_{ij} \quad (9)$$

$$d_{ij}(k+1) = d_{ij}(k) + \Delta d_{ij} \quad (10)$$

According to above equations η_m and η_d denote the learning rates of the translation and dilation of the wavelet layer. As regards, the sensitivity of the system $\frac{\partial P}{\partial u}$ cannot exactly be calculated, an identifier must be implemented to compute the sensitivity of the power system. So at this point to increase the speed of the on-line training, the following equation is used (11):

$$\delta_0 \cong e + e(1 - z^{-1}) \quad (11)$$

D. Convergence analyses of WNN via Adaptive learning rates (ARL)

We now analyze the convergence of the proposed identifier and controller. The convergence of the WNN is related to select the appropriate learning rate. Since the learning rate is an essential factor for determining the performance of the neuro identifier and the neuro controller trained via the back propagation (BP) or gradient descent (GD) method, it is important to find the optimal learning rate [30]. However, in the conventional GD method, it is difficult to choose an appropriate learning rate because the appropriate learning rate is usually selected as a time invariant constant by trial and error. Accordingly, the ALRs, which can adapt rapidly the change of the plant, have been researched for the various neural networks [31,32,33]. Based on this progress about the ALRs, we devise some theorems for the convergence of the proposed indirect adaptive control system.

D.1. Convergence analysis for identification

Let us define a discrete Lyapunov function as:

$$V(k) = E(k) = \frac{1}{2}(e(k))^2 \tag{12}$$

where $e(k)$ is the identification error. The change in the Lyapunov function is obtained by equation (13):

$$\Delta V(k) = V(k + 1) - V(k) = \frac{1}{2}[e^2(k + 1) - e^2(k)] \tag{13}$$

The error difference can be represented by equation (14):

$$\Delta e(k) = e(k + 1) - e(k) \cong \left[\frac{\partial e(k)}{\partial w_i} \right]^T \Delta w_i \tag{14}$$

where W_i is an arbitrary component of the vector W of the WNN and is equal to (15):

$$W = [w, m, d]^T \tag{15}$$

And the corresponding change of W_i is denoted by ΔW_i :

$$\Delta W_i = \eta_w \delta_0 \frac{\partial u}{\partial w_i} \tag{16}$$

Where η_w is an arbitrary diagonal element of the learning rate matrix η_w corresponding to the weight component W_i .

Proposition 1. Let $\eta_w = \text{diag}[\eta_1 \ \eta_2 \ \eta_3] = \text{diag}[\eta_w \ \eta_m \ \eta_d]$ be the learning rates for the weights of the WNN and define C_{max} as:

$$C_{max} = [c_{max}^1, c_{max}^2, c_{max}^3]^T = \left[\max \left\| \frac{\partial u}{\partial w} \right\|, \max \left\| \frac{\partial u}{\partial m} \right\|, \max \left\| \frac{\partial u}{\partial d} \right\| \right]^T \tag{17}$$

In the above equation $\| \cdot \|$ denotes the Euclidean norm and the convergence is guaranteed if η_1 are chosen to satisfy $\eta_w = \lambda / c_{max}^l, l=1,2$ and 3, in which λ is a positive constant gain. Full details are given in appendix B.

Proposition 2. Let η_w be the learning rate for weights w . The convergence of WNN will then be guaranteed if the following learning rate is used:

$$\eta_w = \lambda / N_w \tag{18}$$

In the above equation N_w is the neurons number of the wavelet layer. Full details are given in appendix C.

In order to prove Proposition 3, the following lemmas are used.

Lemma 1. Let $f(t) = t \exp(-t^2)$. Then $|f(t)| < 1 \forall t \in \mathcal{R}$.

Lemma 2. Let $g(t) = t \exp(-t^2)$. Then $|g(t)| < 1 \forall t \in \mathcal{R}$.

Proposition 3. Let η^m and η^d be the learning rates of the translation, and dilation, respectively. The convergence of WNN will then be guaranteed if the following equations are used (19) and (20). The following equations $N_{i,j}/w_{max}$ and $|d|_{min}$ are the input number of the WNN, the maximum of the absolute value of weights vector and the minimum of the

absolute value of dilations vector, respectively. Full details are given in appendix D.

$$\eta_m = \eta_w \left[\frac{|d_{ij}|_{min}}{2|w_j|_{max} \exp(-0.5)} \right]^2 \tag{19}$$

$$\eta_d = \eta_w \left[\frac{|d_{ij}|_{min}}{2|w_j|_{max} \exp(0.5)} \right]^2 \tag{20}$$

IV. RESULTS AND SIMULATIONS

To investigate the performance of the proposed controller, the two-machine power system shown in Fig.2. To show the robustness of the proposed design approach, different operating conditions and contingencies are considered for the system with and without controller. Hence, different loading conditions given in Table 3 are considered. Two different operating conditions (nominal and heavy) are considered and simulation studies are carried out under different fault disturbances and fault clearing sequences. The effectiveness of the performance of the proposed method our trial and error studies show that the controller performance is often similar for sampling rates in the range of (30–100) Hz. Therefore, a sampling frequency of 60 Hz is used in these studies. Further details of the proposed method (OTWNNC) is shown in Table 4.

Table3: Different loading conditions.

Loading conditions	G1[p.u]	G2[p.u]
Nominal Loading	0.95	0.81
Heavy Loading	1	0.99

Table4: The structure of OTWNNC for the simulations

	Number of existing neurons		
	Input layer(N_i)	Wavelet layer(N_w)	Output layer
OTWNN	2	10	1

Case 1: Nominal loading condition, one-phase to ground and three-phase to ground fault

The behavior of the proposed controllers is verified at nominal loading condition under two disturbances. In the first case, a one-phase to ground (L–G) fault is applied at the bus2 at $t=1.1$ s and cleared at $t=1.24$ s. Fig4-a show the response of ΔW_{12} due to this disturbance for light loading condition. According to figure4-a capability of the proposed coordinated controller in reducing the settling time and damping power system oscillations. Moreover, the settling time of these oscillations is $T_s = 2.81$ for proposed method (OTWNNC). So the proposed controller is capable of providing sufficient damping to the system oscillatory modes compared with no controller. Fig 4-b shows the generator rotor angle changes. In the second case, a three-phase to ground (L-L-L–G) fault is applied at the bus1 at $t=1.1$ s and cleared at $t=1.2$ s Fig5-a. It is clear that the performance of proposed controller in damping the oscillations is acceptable. Also, the settling time of these oscillations is $T_s = 3.26$ s for proposed method (OTWNNC).



It can be seen from Fig. 5-b that the first swing in the rotor angle is reduced to $\delta = 52.76$ (with proposed control). Also, the output of OTWNNC and the adaptive learning rates for the three-phase to ground fault are illustrated in Fig. 6.

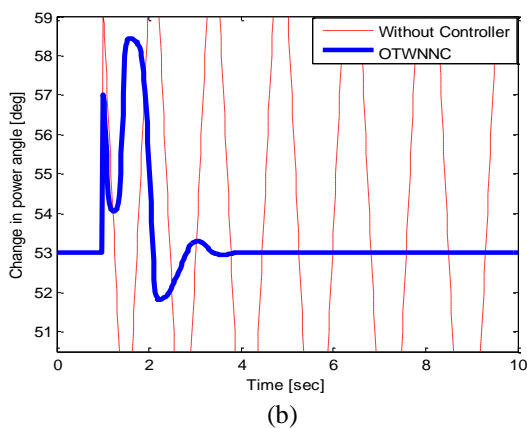
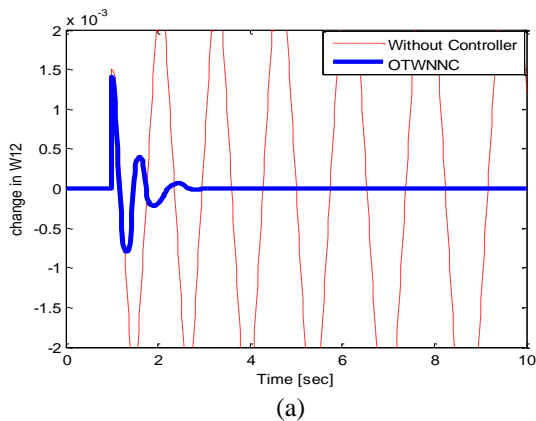


Fig4:The inter-area oscillations for and L-G fault

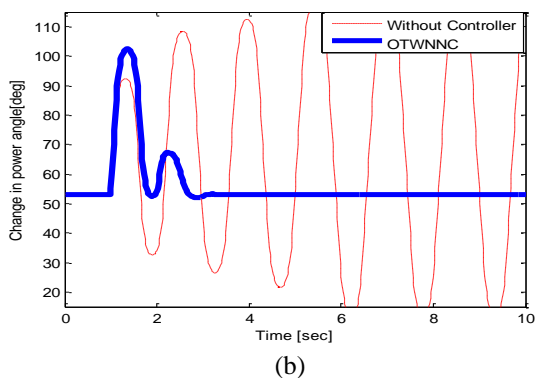
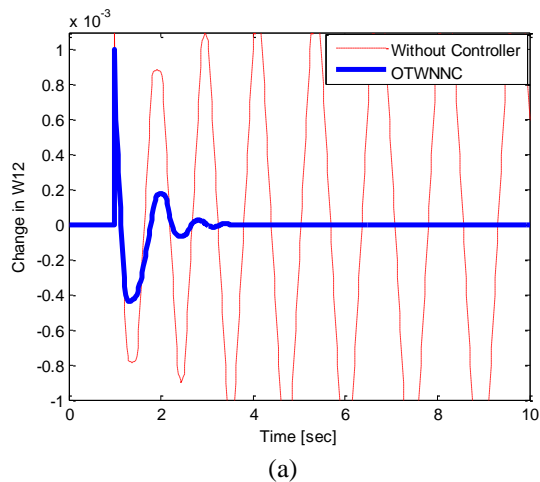


Fig5:The inter-area oscillations L-L-L-G fault

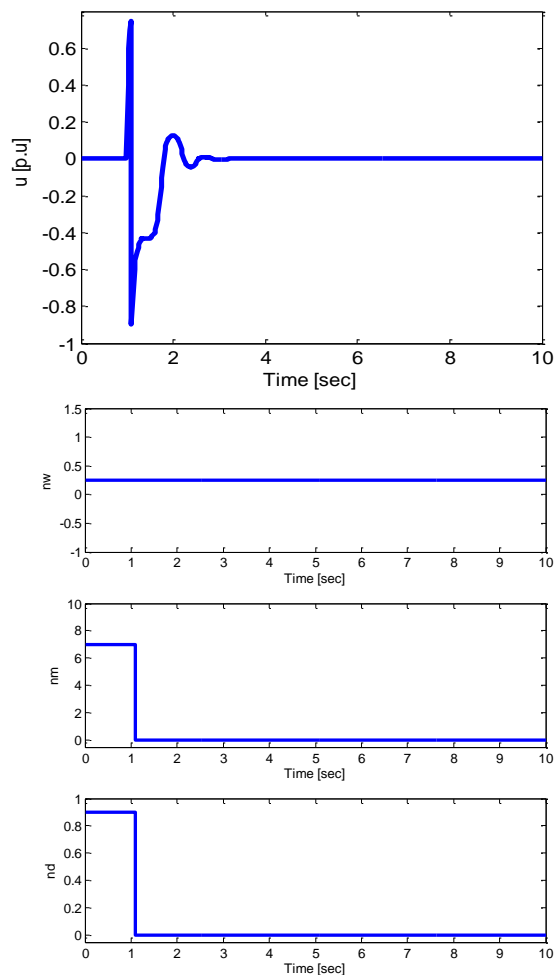
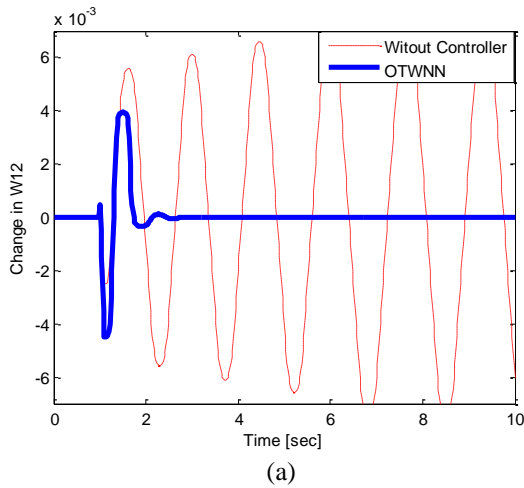


Fig6:The performance of proposed controller L-L-L-G fault.

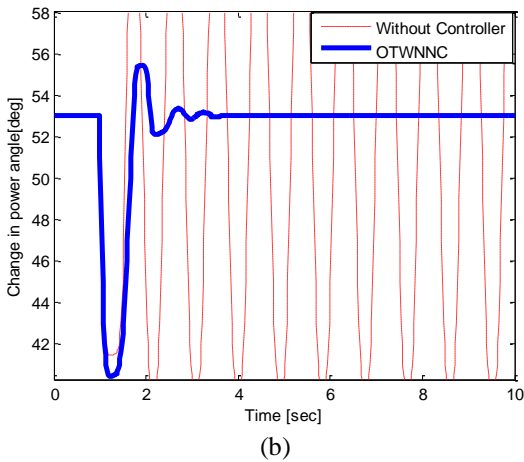
Case 2: Heavy loading condition, two-phase to ground and three-phase to ground fault

The effectiveness of the proposed controllers is also examined at heavy loading condition. In the first case, it is assumed that an L-L-G fault is occurred at bus 3 during 100 ms. The system speed deviation and power angle response under this contingency is shown in Fig. 7a and b, which clearly depicts the robustness of proposed controllers for changes in operating condition and fault location. According to Fig7-a, the settling time of these oscillations is $T_s = 2.73s$ for proposed method (OTWNNC). There is also the power angle is reduced f to $\delta=53.11$ Fig 7-b. In the second case, a three-phase (L-L-L-G) to ground is considered at bus 3 during 140 ms. Fig.8a and b shows the system response for the following contingency. It is clear from the figures that the proposed controller is robust and provides efficient damping even under heavy disturbance conditions. Hence, according to figure8-a it is clear from these figures that the proposed controller attains better performance and supplies superior damping compared with the without controller. The required settling time to diminish these oscillations is nearly 3.36 s for OTWNNC. It can be seen from Fig. 8-b that the first swing in the rotor angle is reduced to $\delta = 52.96$ (with proposed control). Therefore, the designed controller is able to achieve adequate damping to the system oscillatory modes.



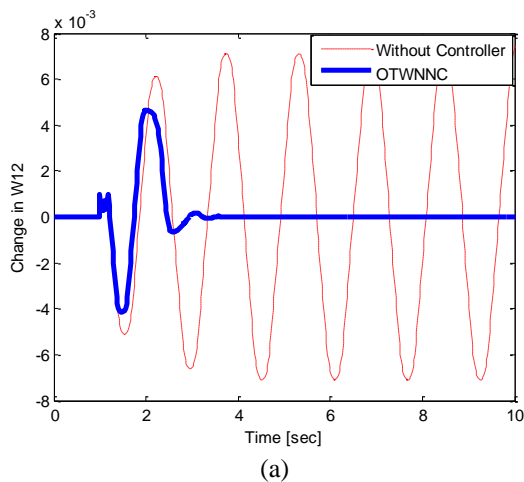


(a)

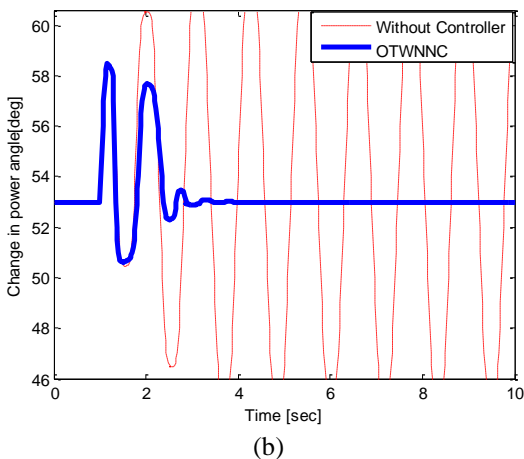


(b)

Fig7:The inter-area oscillations for an L-L-G fault



(a)



(b)

Fig8:The inter-area oscillations for an L-L-L-G fault.

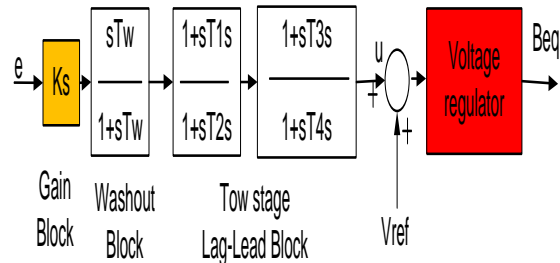


Fig.9.Structure of Lag-Lead compensator.

Case3: A comparative study

To evaluate the effectiveness and robustness of the proposed Controller in improving the transient stability, the performance of the system with the proposed OTWNN controller is compared to with the results obtained from a lag-lead compensator [34].As regards, Lag-lead compensators are widely used in power systems for different objectives because of their simple structure and acceptable performance. Fig. 9 shows the lag-lead compensators structure of the power used in the present study. It consists of a gain block with gain K_s , a signal washout block and two-stage phase compensation block. Hence, the signal washout block serves as a high-pass filter, with the time constant T_w , high enough to allow signals associated with oscillations in input signal to pass unchanged. Without it steady changes in input would modify the output. From the viewpoint of the washout function, the value of T_w is not critical and may be in the range of 1–20 s [35]. The phase compensation blocks (time constants T_{1S} , T_{2S} and T_{3S} , T_{4S}) provide the appropriate phase-lead characteristics to compensate for the phase lag between input and the output signals. Hence, the difference between P_{ref} and P is chosen as the input of lag-lead compensator. $T_w=10$ sand $T_2 =T_4 =0.3$ s are used in this paper. Also, more efficient methods have been used the controller gain K_S and the time constants $T_1 S$ and $T_3 S$ must be determined. So, the Particle Swarm Optimization (PSO) algorithm is used to determine the optimal parameters of lag-lead compensator.PSO parameters are listed in Table 5.

A. Particle Swarm Optimization:

The PSO is a population based stochastic optimization technique developed by Eberhart and Kennedy in 1995. The PSO algorithm is inspired by social behavior of bird flocking or fish schooling. The system is initialized with a population of random solutions and searches for optima by updating generations. However, unlike GA, PSO has no evolution operators such as crossover and mutation. In PSO, the potential solutions, called particles, fly through the problem space by following the current optimum particles. Compared to GA, the advantages of PSO are that PSO is easy to implement and there are few parameters to adjust. PSO has been successfully applied in many areas. The standard PSO algorithm employs a population of particles. The particles fly through the n-dimensional domain space of the function to be optimized. The state of each particle is represented by its position $x_i = (x_{i1}, x_{i2}, \dots, x_{in})$ and velocity $V_i = (v_{i1}, v_{i2}, \dots, v_{in})$, the states of the particles are updated.

The three key parameters to PSO are in the velocity update equation (21). First is the momentum component, where the inertial constant w , controls how much the particle remembers its previous velocity [36].

The second component is the cognitive component. Here the acceleration constant C_1 , controls how much the particle heads toward its personal best position. The third component, referred to as the the social component, draws the particle toward swarm's best ever position; the acceleration constant C_2 controls this tendency. The flow chart of the procedure is shown in Fig 10. Each particle is updated by two "best" values during every iteration. The first one is the position vector of the best solution (fitness) this particle has achieved so far.

$$v_i^{k+1} = wv_i^k + c_1r_1(pb_{best}_i - x_i^k) + c_2r_2(gbest_k - x_i^k) \quad (21)$$

$$x_i^{k+1} = x_i^k + v_i^{k+1} \quad (22)$$

The fitness value $p_i = (p_{i1}, p_{i2}, \dots, p_{in})$ is also stored. This position is called pb_{best} . Another "best" position that is tracked by the particle swarm optimizer is the best position, obtained so far, by any particle in the population. This best position is the current global best $p_g = (p_{g1}, p_{g2}, \dots, p_{gn})$ and is called gb_{best} . At each time step, after finding the two best values, the particle updates its velocity and position according to (21) and (22).

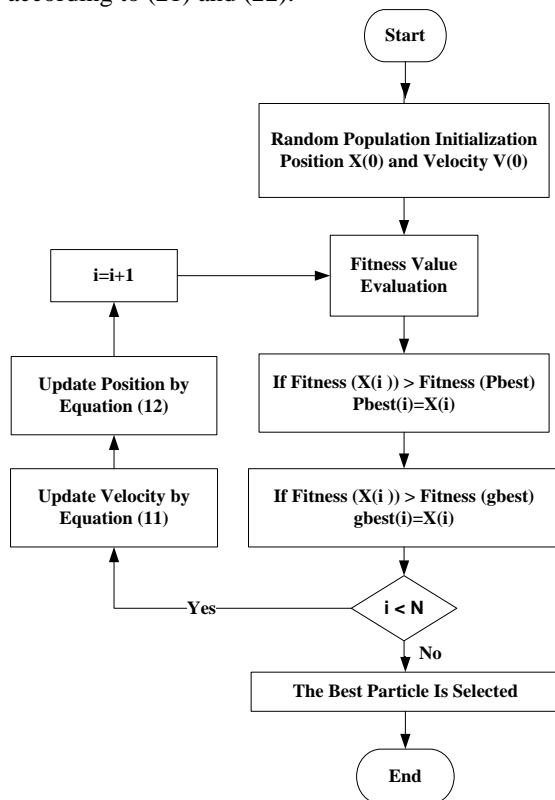


Fig.10:PSO flow chart

Table 5: Parameters used in PSOalgorithm.

Parameters	N_c	c_1	c_2	r_1	r_2
Value	200	2	2	1.05	1

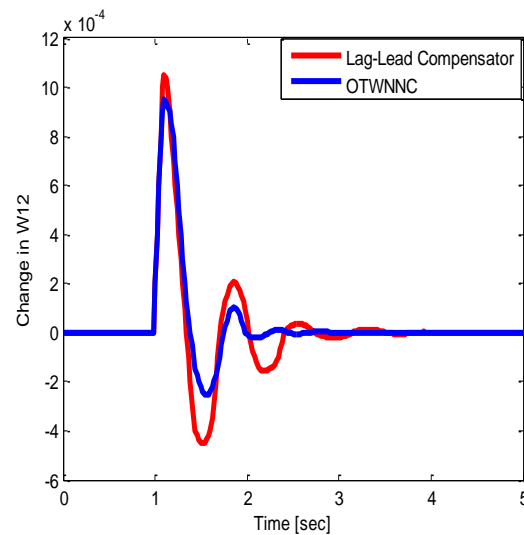
Objective Function:

In this paper, objective function should be minimized by the PSO algorithm to achieve the optimal parameters. The objective function is expressed by the following

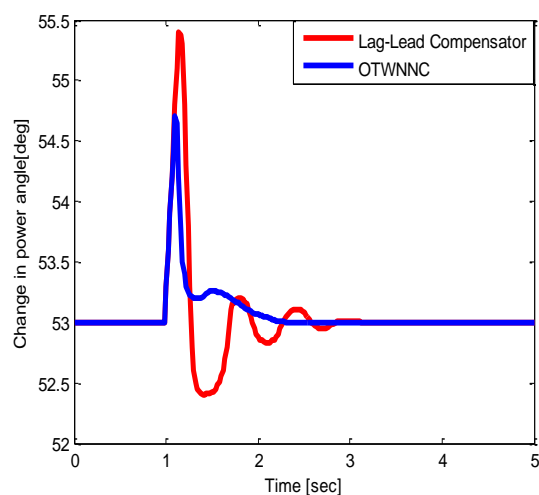
equation(21),in this equation $W1$ and $W2$ are the rotor speed of $M1$ and $M2$; t_{sim} is the time range of simulation. Parameters optimization by PSO algorithms is shown in Table 6.

$$f = \int_0^{t_{sim}} t |w_1 - w_2| dt \quad (21)$$

According to figure 11a and b, it is assumed that an L-L-G fault is occurred at bus 2. The system speed deviation and power angle response under this condition are illustrated in Fig 10a-b. It is obvious from the figures that the proposed OTWNN controller demonstrates better damping Properties to low frequency oscillations and faster stability in comparison with without controller. The settling time are $T_s = 2.76$ and 3.22 s for OTWNNC and Without controller respectively for Fig11-a.Also, it can be seen from Fig. 11-b that the first swing in the rotor angle is reduced from $d = 37.7_$ (without control) to $d = 35.9_$ (with proposed control). Consequently, the power transfer ability as well as the power system stability are increased by way of the proposed OTWNN controller.The convergence of PSO is shown in Fig 12.



(a)



(b)

Fig11:The comparative between OTWNNC and Lag-Lead compensator



Table6:Final optimal values of parameters of lag-lead compensator.

Optimization Value	Parameters of lag-lead compensator		
	k_s	T_{1s}	T_{3s}
	7.26	0.0451	0.1011

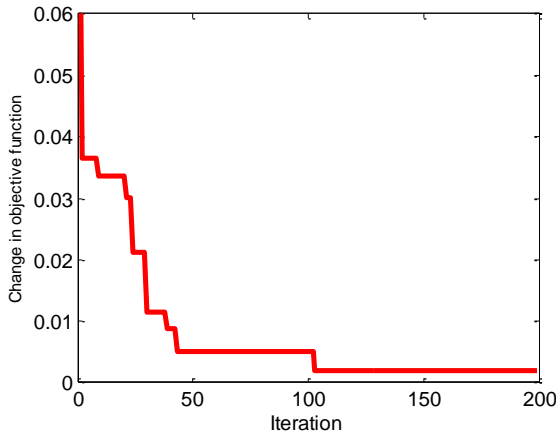


Fig12:The convergence profile PSO

V. CONCLUSIONS

In this study, a new intelligent controller based on wavelet neural network is proposed to control a SVC in order to improve the transient stability in a two-area two-machine power system. In order to achieve the best results for the proposed controller is an online trained wavelet neural network. Using the Lyapunov approach, the convergence theorems for SRWNN have been proven and, from this process, the optimal adaptive learning rates have been established. To further demonstrate the ability of the proposed method, two different loading conditions and with several disturbances are considered. Simulations results assure the effectiveness of the proposed controller in providing good damping characteristic to system oscillations over a wide range of loading conditions and disturbance.

Appendix A

A. Data in Table 1:

r_a , the resistance of stator winding of generators; x_d , the d-axis synchronous reactance of generators; x'_d , the d-axis transient reactance of generators; x''_d , the d-axis sub transient reactance of generators; x_q , the q-axis synchronous reactance of generators; x'_q , the q-axis transient reactance of generators; x''_q , the q-axis sub transient reactance of generators; x_l , the leakage reactance of generators; T'_{do} , the d-axis transient open-circuit time constant; T''_{do} , the d-axis sub transient open-circuit time constant; T'_{qo} , the q-axis subtransient open-circuit time constant; H , the inertia constant.

B. Data in Table 2:

K_a , the gain of the first-order system representing the main regulator; T_a , the time constant of the first-order system representing the main regulator; K_e , the gain of the first-order system representing the exciter; T_e , the time constant of the first-order system representing the exciter; K_f , the gain of the first-order system representing a derivative feedback; T_f , the time constant of the first-order system representing derivative feedback; E_{fmax} , the upper limit of regulator output; E_{fmin} , the lower limit of regulator output.

Appendix B.

From Eq.(12), $V(k) > 0$. Using Eq.(14), we can obtain:

$$e(k+1) = e(k) + \left[\frac{\partial e(k)}{\partial w_i} \right]^T \Delta w_i \quad (14)$$

$$e(k+1) = e(k) - \left[\frac{\delta_0}{e(k)} \frac{\partial u}{\partial w_i} \right]^T \eta_w \delta_0 \frac{\partial u}{\partial w_i}$$

$$\|e(k+1)\| = \left\| e(k) \left[1 - \eta_w \left(\frac{\delta_0}{e(k)} \right)^2 \left(\frac{\partial u}{\partial w_i} \right)^T \frac{\partial u}{\partial w_i} \right] \right\|$$

$$= \|e(k)\| \left\| \left[1 - \eta_w \left(\frac{\delta_0}{e(k)} \right)^2 \left(\frac{\partial u}{\partial w_i} \right)^T \frac{\partial u}{\partial w_i} \right] \right\| = \|e(k)\| \gamma$$

$$\text{Where: } \gamma = \left\| \left[1 - \eta_w \left(\frac{\delta_0}{e(k)} \right)^2 \left(\frac{\partial u}{\partial w_i} \right)^T \frac{\partial u}{\partial w_i} \right] \right\|$$

$$= \left\| \left[1 - \eta_w \left(\frac{\delta_0}{e(k)} \right)^2 (c_{max}^l)^2 \right] \right\| \quad (A)$$

From Eq.(A) and using Eq.(13):

if $\left\| 1 - \eta_w (\delta_0 / e(k))^2 c_{max}^l \right\| < 1$ is satisfied, then the convergence of the WNN can be guaranteed. Therefore, we can calculate $\eta_w = \lambda / (c_{max}^l)^2$ $l=1,2$ and 3 .

Appendix C.

$c^1 = \frac{\partial u}{\partial w} = \Phi$, where $\Phi = [\Phi_1, \Phi_2, \dots, \Phi_{N_w}]^T$ is the output vector of the wavelet layer of the WNN. Then, because we have $\Phi_j \leq 1$ for all j , $\|c^1(k)\| \leq \sqrt{N_w}$. So, we can calculate $\eta_w = \lambda / N_w$.

Appendix D.

$$c^2 = \frac{\partial u}{\partial m_{ij}} = w_j = \left(\frac{\partial \Phi_j}{\partial m_{ij}} \right) \leq |w_j| \left\{ \max \left[\left| \frac{\partial \Phi_j}{\partial m_{ij}} \right| \right] \right\}$$

$$= |w_j| \left\{ \max \left[\left| \frac{\partial \Phi_j}{\partial net_j} \frac{\partial net_j}{\partial m_{ij}} \right| \right] \right\}$$

$$\leq |w_j| \left\{ \max \left[\left| \frac{-2 \exp(-0.5)}{d_{ij}} \right| \left| \left[\frac{1}{2} \left(\frac{x_i - m_{ij}}{d_{ij}} \right)^2 \right] \right| \right. \right.$$

$$\left. \left. - \frac{1}{2} \exp \left\{ - \left[\frac{1}{2} \left(\frac{x_i - m_{ij}}{d_{ij}} \right)^2 - \frac{1}{2} \right] \right\} \right| \right] \right\}$$

$$\leq |w_j| \left\{ \max \left[\left| \frac{-2 \exp(-0.5)}{d_{ij}} \right| \right] \right\} = |w_j| \left(\frac{2 \exp(-0.5)}{|d_{ij}|_{min}} \right)$$

$$\text{Tuse: } \|c^2\| < \sqrt{N_w} |w_j|_{max} \left(\frac{2 \exp(-0.5)}{|d_{ij}|_{min}} \right)$$

Then we have:

$$\eta_m = \eta_w \left[\frac{|d_{ij}|_{min}}{2 |w_j|_{max} \exp(-0.5)} \right]^2$$

Since:

$$c^3 = \frac{\partial u}{\partial d_{ij}} = w_j \left(\frac{\partial \Phi_j}{\partial d_{ij}} \right) \leq |w_j| \left\{ \max \left[\left| \frac{\partial \Phi_j}{\partial net_j} \frac{\partial net_j}{\partial d_{ij}} \right| \right] \right\}$$

$$\leq |w_j| \left\{ \max \left[\left| \frac{2 \exp(0.5)}{d_{ij}} \right| \left| \left(\frac{x_i - m_{ij}}{d_{ij}} \right) \exp \left[- \left(\frac{x_i - m_{ij}}{d_{ij}} \right)^2 \right] \right| \right| \left[\frac{1}{2} \right. \right.$$

$$\left. \left. - \frac{1}{2} \left(\frac{x_i - m_{ij}}{d_{ij}} \right)^2 \right] \exp \left\{ - \left[\frac{1}{2} \left(\frac{x_i - m_{ij}}{d_{ij}} \right)^2 - \frac{1}{2} \right] \right\} \right. \right.$$

$$\left. \left. - \frac{1}{2} \left(\frac{x_i - m_{ij}}{d_{ij}} \right)^2 \right] \right] \right\}$$

$$\leq |w_j| \left\{ \left[\left| \frac{2 \exp(0.5)}{d_{ij}} \right| \right] \right\} = |w_j| \left(\frac{2 \exp(0.5)}{|d_{ij}|_{min}} \right)$$

$$\text{Thus: } \|c^3\| < \sqrt{N_w} |w_j|_{max} \left(\frac{2 \exp(0.5)}{|d_{ij}|_{min}} \right)$$

Then, we have:

$$\eta_a = \eta_w \left[\frac{|d_{ij}|_{\min}}{2|w_j|_{\max} \exp(0.5)} \right]^2$$

REFERENCES

- [1] P. Kundur, J. Paserba, V. Ajjarapu, G. Andersson, A. Bose, C. Canizares, N. Hatziairgiou, D. Hill, A. Stankovic, C. Taylor, T. Cutsem, and V. Vittal, "Definition and classification of power system stability," *IEEE Trans. Power Syst.*, vol. 19, no. 2, pp. 1387–1401, May 2004.
- [2] J. J. Sanchez-Gasca, "Coordinated control of two FACTS devices for damping interarea oscillations," *IEEE Trans. Power Syst.*, vol. 13, no. 2, pp. 428–434, May 1997.
- [3] R. Mohan, Mathur and R. K. Varma, *Thyristor-Based FACTS Controller For Electrical Transmission System*. Piscataway, NJ: IEEE Press/Wiley Interscience, 2002.
- [4] K. Clark, B. Fradaneesh, and R. Adapa, "Thyristor-controlled series compensation application study—Control interaction considerations," *IEEE Trans. Power Del.*, vol. 10, no. 2, pp. 1031–1037, Apr. 1995.
- [5] D. P. He, C. Y. Chung, and Y. Xue, "An eigenstructure-based performance index and its application to control design for damping interarea oscillations in power systems," *IEEE Trans. Power Syst.*, vol. 26, no. 4, pp. 2371–2380, Nov. 2011.
- [6] Y. C. Chang, R. F. Chang, T. Y. Hsiao, and C. N. Lu, "Transmission system locability enhancement study by ordinal optimization method," *IEEE Trans. Power Syst.*, vol. 26, no. 1, pp. 451–459, Feb. 2011.
- [7] X. Tan, N. Zhang, L. Tong, and Z. Wang, "Fuzzy control of thyristorcontrolled series compensator in power system transients," *Fuzzy Sets Syst.*, vol. 110, pp. 429–436, 2000.
- [8] X. Lei, E. N. Lerch, and D. Povh, "Optimization and coordination of damping controls for improving system dynamic performance," *IEEE Trans. Power Syst.*, vol. 16, no. 3, pp. 473–480, Aug. 2001.
- [9] N. Mithulananthan, C. A. Canizares, J. Reeve, and G. J. Rogers, "Comparison of PSS, SVC, and STATCOM controllers for damping power system oscillations," *IEEE Trans. Power Syst.*, vol. 18, no. 2, pp. 786–792, May 2003.
- [10] M. E. Aboul-El, A. A. Sallam, J. D. McCalley, and A. A. Fouad, "Damping controller design for power system oscillations using global signals," *IEEE Trans. Power Syst.*, vol. 11, no. 2, pp. 767–773, May 1996.
- [11] U. P. Mhaskar and A. M. Kulkarni, "Power oscillation damping using FACTS devices: Model controllability, observability in local signals, and location of transfer function zeros," *IEEE Trans. Power Syst.*, vol. 21, no. 1, pp. 285–294, Feb. 2006.
- [12] A. M. Simões, D. C. Savelli, P. C. Pellanda, N. Martins, and P. Apkarian, "Robust design of a TCSC oscillation damping controller in a weak 200-kv interconnection considering multiple power flow scenarios and external disturbances," *IEEE Trans. Power Syst.*, vol. 24, no. 1, pp. 226–236, Feb. 2009.
- [13] B. Chaudhuri, S. Ray, and R. Majumder, "Robust low-order controller design for multi-modal power oscillation damping using flexible AC transmission system devices," *IET Gener. Transm. Distrib.*, vol. 3, no. 5, pp. 448–459, 2009.
- [14] J. M. González, C. A. Cañizares, and J. M. Ramoirez, "Stability modeling and comparative study of series vectorial compensators," *IEEE Trans. Power Del.*, vol. 25, no. 2, pp. 1093–1103, Apr. 2010.
- [15] P. K. Dash, S. Morris, and S. Mishra, "Design of a nonlinear variable gain fuzzy controller for FACTS devices," *IEEE Trans. Control Syst. Technol.*, vol. 12, no. 3, pp. 428–438, May 2004.
- [16] C. F. Lu and C. F. Juang, "Evolutionary fuzzy control of flexible AC transmission system," *Proc. Inst. Elect. Eng., Gener., Transm., Distrib.*, vol. 152, no. 4, pp. 441–448, Jul. 2005.
- [17] Y.L. Abdel-Magid, M.A. Abido, "Optimal Multi objective Design of Robust Power System Stabilizers using Genetic Algorithms", *IEEE Trans. On Power Systems*, Vol. 18, pp. 1125-1132, 2003.
- [18] K. Sebaa, M. Boudour, "Optimal Locations and Tuning of Robust Power System Stabilizer Using Genetic Algorithms", *Electric Power Systems Research*, Vol. 79, pp. 406-416, 2006.
- [19] S. Mishra, M. Tripathy, J. Nanda, "Multi-Machine Power System Stabilizer by Rule Based Bacteria Foraging", *Electric Power Systems Research*, Vol. 77, pp. 1595-1607, 2007.
- [20] H. Shayeghi, H.A. Shayanfar and A. Ghasemi, "A Robust ABC Based PSS Design for a SMIB Power System", *International Journal on Technical and Physical Problems of Engineering (IJTPE)*, Issue 8, Vol. 3, No. 3, pp. 86-92, September 2011.
- [21] M.A. Abido, "A Novel Approach to Conventional Power System Stabilizer Design Using Tabu Search", *Electrical Power and Energy Systems*, Vol. 21, pp443- 454, 1999.
- [22] A.M. El-Zonkoly, A.A. Khalil, N.M. Ahmied, "Optimal Tuning of Lead-Lag and Fuzzy Logic Power System Stabilizers using Particle Swarm Optimization", *Expert Systems with Applications*, Vol. 36, pp. 2097- 2106, 2009.
- [23] H.M. Soliman, E.H.E. Bayoumi, M.F. Hassan, "PSO-Based Power System Stabilizer for Minimal Overshoot and Control Constraints", *Journal of Electrical Engineering*, Vol. 59, No. 3, pp. 153-159, 2008.
- [24] A. Safari, H. Shayeghi, H.A. Shayanfar, "Optimization Based Control Coordination of STATCOM and PSS Output Feedback Damping Controller Using PSO Technique", *International Journal on Technical and Physical Problems of Engineering (IJTPE)*, Issue 5, Vol. 2, No. 4, pp. 6-12, December 2010.
- [25] H. Shayeghi, A. Ghasemi, "Application of PSO TV to Improve Low Frequency Oscillations", *International Journal on Technical and Physical Problems of Engineering (IJTPE)*, Issue 9, Vol. 3, No. 4, pp. 36-44, December 2011.
- [26] A. Alfi, M. Khosravi, "Optimal power system stabilizer design TO reduce low frequency oscillation via an improved swarm optimization algorithm", *International Journal on Technical and Physical Problems of Engineering (IJTPE)*, Issue 11, Vol. 4, No. 2, pp. 24-33, June 2012.
- [27] M. J. Laubenberg, M. A. Pai, and K. R. Padiyar, "Hopf Bifurcation Control in Power System with Static Var Compensators," *Int. J. Electric Power and Energy Systems*, Vol. 19, No. 5, pp. 339–347, 1997.
- [28] N. Mithulananthan, C. A. Canizares, and John Reeve, "Hopf Bifurcation Control in Power System Using Power System Stabilizers and Static Var Compensators," *Proc. of NAPS'99*, pp. 155–163, San Luis Obispo, California, Oct. 1999.
- [29] S. Haykin, *Neural Networks: A Comprehensive Foundation*. New York: Macmillan, 1994.
- [30] G.D. Magoulas, M.N. Vrahatis, G.S. Androulakis, Improving the convergence of the backpropagation algorithm using learning rate adaptation methods, *Neural Computation* 11 (1999) 1769–1796.
- [31] C.C. Ku, K.Y. Lee, Diagonal recurrent neural networks for dynamics systems control, *IEEE Trans. Neural Networks* 6 (1) (1995) 144–156.
- [32] C.H. Lee, C.C. Teng, Identification and control of dynamic systems using recurrent fuzzy neural network, *IEEE Trans. Fuzzy Systems* 8 (4) (2000) 349–366.
- [33] J. Yoo, J.B. Park, Y.H. Choi, Direct adaptive control using self recurrent wavelet neural network via adaptive learning rates for stable path tracking of mobile robots, in: *Proc. American Control Conference*, 2005, pp. 288–293.
- [34] Panda, Sidhartha, 2009. Multi-objective evolutionary algorithm for SSSC-based controller design. *Electr. Power Syst. Res.* 79 (6), 937–944.
- [35] Kundur P. *Power system stability and control*. McGraw-Hill; 1994.
- [36] Y. Shi and R. Eberhart, "A modified particle swarm optimizer," *Proc. Int. Conf. on Evolutionary Computation*, Anchorage, pp. 69–73, 1998, AK, USA.

Mohsen Darabian received his B.Sc. degree in Electrical from Azad university of Abhar branch, Iran, in 2010. He is currently an MSc student at Department of Power Engineering, University of Zanjan, Zanjan, Iran. His research interests include application of intelligent methods in power systems, distributed generation modeling, power electronic, FACTS, power quality and power system dynamics.

Bahram KHorram was born in Zanjan, Iran, in 1982. He received the B. Sc degree in Electrical from Azad university of Abhar branch, Iran, in 2008. He is currently an MSc student at Department of Power Engineering, University – South Tehran branch, Iran. His research interests include application of intelligent methods in, power system dynamics, FACTS devices and IEC standards.

Mehdi Azari was born in Zanjan, Iran in 1986. He received his B.Sc. degree in electrical engineering from University of Zanjan, Zanjan, Iran, in 2008. He is currently an MSc student at Department of Electrical Engineering, University of Zanjan, Zanjan, Iran. His research interests include application of intelligent methods in power systems, distributed generation modeling, power system protection and control and digital protective relays.

